Surface atomic and electronic structure of cassiterite SnO_2 (110)

T. J. Godin and John P. LaFemina
Molecular Science Research Center, Pacific Northwest Laboratory, P.O. Box 999, Richland, Washington 99352
(Received 17 June 1992)

Using a tight-binding, total-energy model, we have calculated relaxed surface atomic positions, surface-state energies, and densities of states for the reduced and stoichiometric (110) surfaces of rutile-structure tin dioxide (cassiterite). Both relaxed surfaces display a small rumple of the top atomic layer and smaller counter-rumples of the subsurface layers. The surface-state energy lowering caused by the relaxation is small because of the surface topology, which forbids bond-length-conserving motions of the surface atoms. The density of states for the reduced surface agrees qualitatively with photoemission data that indicate the absence of surface states in the fundamental gap of the material.

I. INTRODUCTION

Cassiterite (rutile-structure SnO_2) is a wide-band-gap semiconductor that has many uses where its surface properties play a key role. For example, it has long been used in oxidation catalysis;[1,2] its ability to undergo gas-induced conductivity changes makes it useful in chemical sensor[3–5] applications.

Tin dioxide crystallizes in the rutile structure [Fig. 1(a)], which has tetragonal, D_{4h}^{14} symmetry. There are two formula units per primitive unit cell, with the threefold-coordinated oxygen atoms forming distorted octahedra about the tin atoms.[6] Figure 1(b) shows the bulk first Brillouin zone.

The shaded region in Fig. 1(a) is a (110) cleavage plane, and comprises one surface primitive unit cell. The (110) surfaces of cassiterite are, experimentally, the best characterized. Like many mineral oxides, SnO_2 does not cleave well, but fractures. Moreover, the stoichiometry (i.e., the ratio of tin to oxygen atoms) of cassiterite (110) surfaces is sensitive to the processing conditions under which the surface is prepared. Structurally, there are several ways of terminating the surface shown in Fig. 1(a), each leading to a different surface stoichiometry. Two such terminations are shown in Fig. 2. The first [Fig. 2(a)] consists of a surface layer with two oxygen and two tin atoms (the "reduced" surface). The threefold-

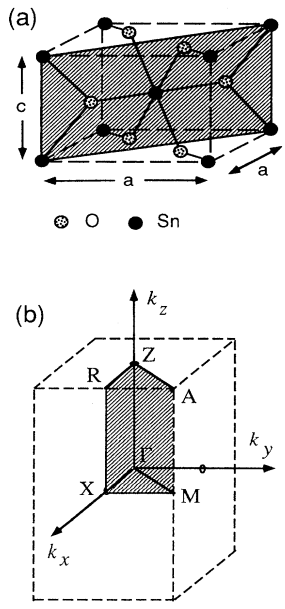

FIG. 1. (a) Primitive unit cell of the bulk cassiterite (rutile) structure. The shaded region is a (110) cleavage plane. (b) First Brillouin zone for this structure, showing high-symmetry points. The shaded region is the irreducible part of the Brillouin zone.

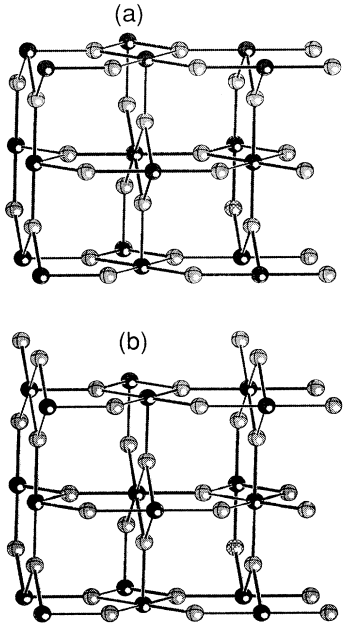

FIG. 2. Ideal (truncated bulk) structures of the (a) reduced and (b) stoichiometric (110) surfaces of cassiterite. The darker balls represent tin atoms and the lighter balls oxygen atoms. The two surfaces differ in that the second has bridging oxygen atoms.

coordinated oxygen atoms each bond to three surface tin atoms which, in turn, have two distinct configurations (fourfold and fivefold coordinated). The second surface [Fig. 2(b)] has one added twofold-coordinated bridging oxygen atom per surface unit cell (the "stoichiometric" surface). The fourfold-coordinated tin atoms of the reduced surface become octahedrally coordinated, like the bulk tin atoms, when these bridging oxygen atoms are added. (The other distinct surface tin atom remains fivefold coordinated, as in the reduced surface.) A third possible termination, with additional, singly coordinate oxygen atoms placed directly above surface tin atoms, will not be considered here.

Experimentally, cassiterite (110) surfaces can have partial occupation of the bridging oxygen sites. Experimental low-energy, electron-diffraction (LEED) and Auger studies of SnO_2 (110) have shown that the surface tin to oxygen ratio can vary from 0.49 to 0.76 depending on the annealing temperature, and that the surface can display $p(1\times1)$, $c(1\times1)$, $p(4\times2)$, $p(4\times1)$, or amorphous structures.[7] To date, there have been no reported quantitative experimental determinations of the atomic structure of either the reduced or stoichiometric surfaces. Recently, however, Cox and co-workers have developed techniques for producing nearly perfect, stoichiometric SnO_2 (110) surfaces,[8,9] which should allow quantitative experimental studies of the relaxed surface geometric and electronic structure of this surface.

The electronic structure of the ideal (unrelaxed truncated bulk) reduced surface was found previously using a tight-binding model.[10] However, there have so far been no quantitative theoretical or computational studies of the atomic geometry or electronic structure of the relaxed stoichiometric or reduced SnO_2 (110) surface.

This paper describes results of tight-binding, total-energy calculations of the relaxed surface geometric and electronic structure of both reduced and stoichiometric cassiterite (110). Both surfaces show a small rumple of the relaxed surface layer, and smaller counter-rumples of the subsurface layers. The relaxed surface electronic states, however, are only slightly lower in energy than those of the unrelaxed surfaces. The calculated densities of states agree qualitatively with photoemission experiments.[11]

We begin by discussing the tight-binding, total-energy model used in the calculations. The results for surface geometric and electronic structure are then examined in detail. The paper concludes with a summary.

II. THE TIGHT-BINDING, TOTAL-ENERGY MODEL

The tight-binding, total-energy model used in this study separates the total energy of a tin dioxide sample into a "band-structure" energy, E_{bs}, that describes the valence electrons, and an interatomic repulsive potential U:

$$E_{tot}=E_{bs}+U \ . \tag{1}$$

E_{bs} is a sum of the occupied eigenvalues of a single-electron, Slater-Koster[12] Hamiltonian integrated over the reduced Brillouin zone. The integration is performed using the quadrature scheme of Chadi and Cohen,[13] using a single node, or "special" point, in k space. U consists of interatomic pair potentials, described below.

To reproduce the bulk SnO_2 band structure, the tight-binding Hamiltonian must include oxygen-oxygen interactions, and must therefore go beyond a nearest-neighbor model.[14] Electronic parameters in the Hamiltonian were taken from a previous study of the bulk SnO_2 band structure,[14] and modified[15] so that the off-diagonal elements scale as d^{-2}, where d is the interatomic spacing.[16] Nearest-neighbor (tin-oxygen) and second- through fourth-nearest-neighbor (oxygen-oxygen) parameters are included, and all oxygen-oxygen interactions are identical (up to a d^{-2} scaling factor). This scheme adequately reproduces the bulk SnO_2 band structure, as shown in Fig. 3.

The repulsive potential U in Eq. (1) is modeled using a power law in the interatomic separations:

$$U=\sum_{i,j} c_1 \left[\frac{r_{1,ij}}{r_{1,0}}\right]^n+\sum_{k,l} c_2 \left[\frac{r_{2,kl}}{r_{2,0}}\right]^n . \tag{2}$$

$r_{1,0}$ and $r_{2,0}$ are, respectively, the nearest tin-oxygen and oxygen-oxygen distances, $r_{1,ij}$ is the distance between tin atom i and oxygen atom j, and $r_{2,kl}$ is the distance between oxygen atoms k and l. The indices i and j run over nearest-neighbor pairs, while k and l run over second- through fourth-nearest neighbors. The constants c_1, c_2, and n are determined by requiring that the model reproduce the correct bulk lattice constant and modulus, and also by requiring that the strength of the repulsion between oxygen atoms at the sum of their covalent radii be comparable to that of the tin-oxygen repulsion at the bulk Sn-O separation distance. In practice, the latter constraint significantly affects c_2 only. This *ad hoc* method of determining c_2 is not critical, however. This is because the distant-neighbor oxygen-oxygen interactions are much weaker than those between the nearest-neighbor tin and oxygen atoms, so that the elastic and structural properties of the model are not very sensitive

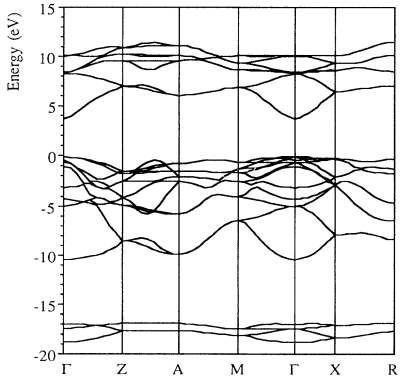

FIG. 3. Bulk tight-binding band structure of cassiterite found using the modified electronic parameters described in Sec. II. The energy scale is set so that the valence-band maximum is at 0 eV. The conduction-band minimum is therefore at 3.8 eV.

to the magnitude of the second term in Eq. (2).[15] The effect of this term is simply to prevent oxygen atoms from approaching each other too closely. For SnO_2, we obtain values of -14.6968, 0.200 59, and 0.000 102 for n, c_1, and c_2, respectively.

The scalings of both the band structure and repulsive terms of Eq. (1) with interatomic distance are important features of the model. They can be justified by general arguments,[16] and facilitate the calculation of the total energy as a function of atomic positions. Moreover, use of the scaling relationships to describe the different oxygen-oxygen interactions reduces the number of required free parameters.

We model the SnO_2 (110) surface by slabs six atomic layers thick, infinite and periodic in directions transverse to the surface plane. Since reconstructions of perfect, clean SnO_2 (110) surfaces are expected to have (1×1) symmetry,[7] it is sufficient to use a single primitive surface unit cell in the model.

Surface relaxations are found by applying Eq. (1) to these slabs, and minimizing the resultant total energy by minimization of the Hellman-Feynman forces[17] on each atom. Surface bound states and resonances are identified by examining the spatially resolved probability densities of the electronic Hamiltonian eigenvectors for the slab.

This tight-binding, total-energy methodology has been applied to a wide variety of materials. In virtually all cases, it reproduces surface atomic geometries[18] to within the experimental uncertainties of low-energy, electron-diffraction measurements (typically 0.05 Å for distances normal to the surface plane and 0.2 Å for distances along the plane).[19] We expect the results of the SnO_2 surface structure calculation to have similar accuracy.

III. RELAXED SURFACE ATOMIC STRUCTURE OF SnO_2(110)

When allowed to relax, both the reduced and stoichiometric surfaces undergo a small rumple of the surface layer, in which both surface tin atoms remain approximately in bulk positions, while the surface-layer oxygen atoms move out from the surface (Fig. 4). There is a much smaller, but significant, "counter-rumple" of the second layer, while third-layer atoms remain approximately in bulk positions.

All relaxations preserve the mirror symmetries of the truncated bulk surface unit cell. This allows the relaxed surface structure to be described by a relatively small number of independent structural parameters, which are shown schematically in Fig. 5. The energy-minimized values of these parameters for both the relaxed and stoichiometric relaxed surfaces are given in Table I.

The parameters of Fig. 5 follow the ordinary conventions of semiconductor surface nomenclature,[18] modified to describe the more complicated rutile (110) surface. Parameters denoted by "Δ" refer to intralayer interatomic distances. The first subscript of "Δ" gives the number of the layer (with the surface layer numbered one, the first subsurface layer two, etc.). The symbol "$\perp$" indicates a projection of the interatomic separation along an axis perpendicular to the surface, while "y" indicates projec-

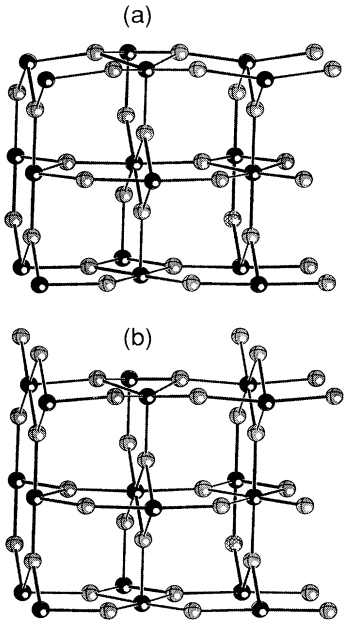

FIG. 4. Relaxed atomic structures of the (a) reduced and (b) stoichiometric (110) surfaces of cassiterite. As in Fig. 2 (unrelaxed surfaces), the darker balls represent tin atoms and the lighter balls oxygen atoms. The atomic positions shown are described quantitatively in Table I.

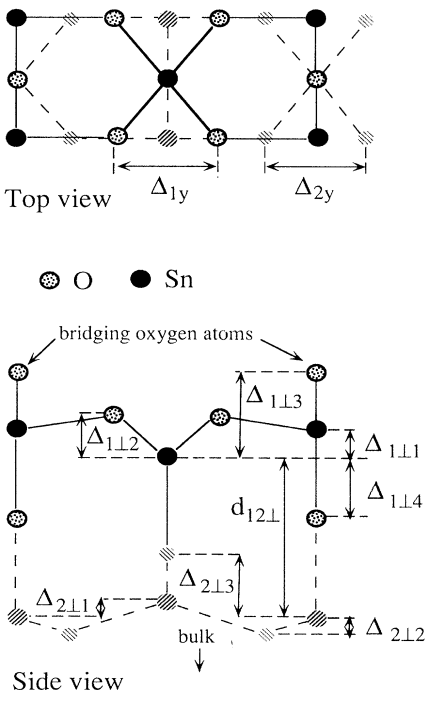

FIG. 5. Definition of independent structure parameters which describe the relaxation of the cassiterite (110) surface. The shaded atomic symbols represent atoms in subsurface layers.

TABLE I. Structure parameters for the ideal (unrelaxed truncated bulk), relaxed reduced, and relaxed stoichiometric surfaces. The parameters are defined in Fig. 5. All units are angstroms.

	$\Delta_{1\perp1}$	$\Delta_{1\perp2}$	$\Delta_{1\perp3}$	$\Delta_{1\perp4}$	Δ_{1y}	Δ_{2y}	$d_{12\perp}$	$\Delta_{2\perp1}$	$\Delta_{2\perp2}$	$\Delta_{2\perp3}$
Ideal	0.00	0.00	1.30	−1.30	2.60	2.60	−3.35	0.00	0.00	1.30
Reduced	−0.05	0.28		−1.29	2.58	2.57	−3.35	0.03	0.08	1.31
Stoichiometric	0.10	0.29	1.37	−1.18	2.53	2.57	−3.24	−0.08	0.00	1.20

tion along an axis parallel to the surface. The final subscript distinguishes independent displacements. Parameters denoted by "d" represent distances between atoms in different layers, with the two numeric subscripts representing the two layers to which those atoms belong.

The relaxations of both the reduced and stoichiometric surfaces can be understood by considering how the oxygen atoms try to rehybridize from their bulk configuration, which is approximately sp^2 plus a nonbonding, lone-electron pair. For the reduced surface the oxygen atoms, in an effort to lower their electronic energies, attempt to move out from the surface into a more tetrahedral (sp^3) configuration about the fourfold coordinated tin atoms. The oxygen atoms cannot fully rehybridize, however, because of the large local strain field (i.e., the large energy cost associated with the significant accompanying changes in bond lengths). For the stoichiometric surface, the twofold coordinated bridging oxygen atoms already exist in approximate sp^3 environments, and thus cannot substantially lower their energies in this way. The Sn-O-Sn bond angle for the relaxed structure (approximately 102°) is thus unchanged from the bulk value.

Currently, there are no quantitative experimental results (e.g., from LEED intensity analyses) that describe the relaxed SnO_2 (110) surface atomic positions. The relaxed surface atomic positions given in Table I differ from the truncated bulk values by distances greater than the resolution of conventional LEED analysis (approximately 0.05 Å normal to the surface plane[19]). The surface relaxations should therefore be observable by LEED experiments.

IV. RELAXED SURFACE ELECTRONIC STRUCTURE OF SnO_2(110)

Figure 6 shows the calculated electronic densities of states for the relaxed slab models of the reduced and stoichiometric surfaces. In both panels of Fig. 6, the lowest curve represents the raw calculated density of states for the six-layer slabs, while the next higher curve represents the same data with peaks Gaussian broadened with a half-width of 0.3 eV.

Figure 6(b) compares the calculated density of states to the results of ultraviolet-photoelectron-spectroscopy (UPS) experiments on the stoichiometric (110) surface.[11] Comparison to the calculated density of states must be made with care, since the experiment includes effects which are not included in the calculation. For example, electron scattering is limited by electron-photon cross-section effects,[20] which are difficult to calculate for electrons in the upper valence band. Moreover, the experimental intensity includes electrons scattered by secondary electron-electron interactions. This skews the intensity distribution towards lower energies.[21] The importance of the comparison in Fig. 6(b), however, is that the qualitative agreement of the experimental and computational results demonstrates that the selected electronic parameters adequately reproduce the electronic structure.

Figure 7 shows the calculated reduced and stoichiometric relaxed (110) surface electronic structures, along with the projected bulk bands, as a function of selected k-space vectors in the reduced surface Brillouin

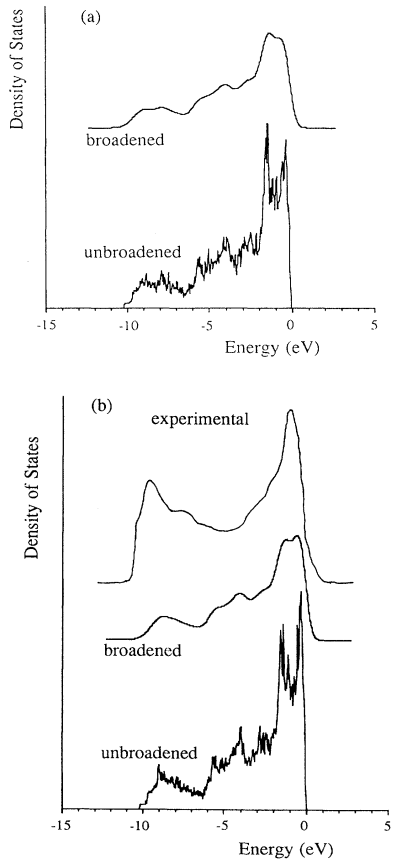

FIG. 6. Calculated densities of states for the (a) reduced and (b) stoichiometric slab models described in Sec. IV. The lower two curves in both panels represent the raw calculated density of states (labeled "unbroadened"), and the same data after Gaussian broadening ("broadened"). The experimental photoemission results of Ref. 11 are shown as the uppermost curve in the second panel (labeled "experimental").

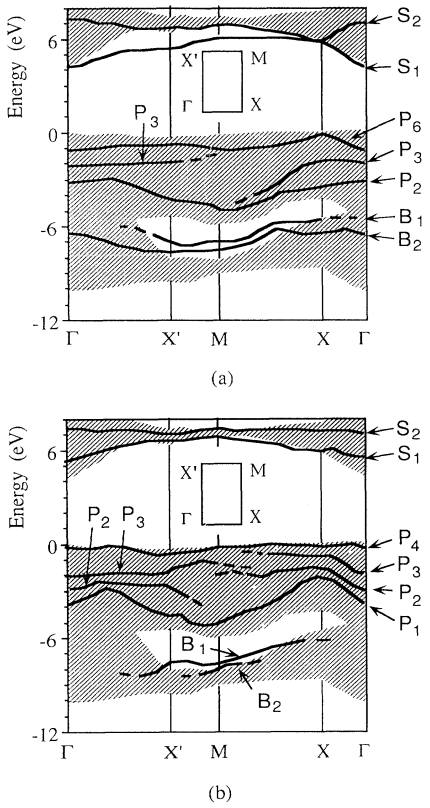

FIG. 7. Surface bound states and resonances of the (a) reduced and (b) stoichiometric (110) surfaces. The shaded regions indicate the projections of the bulk band structure. Orbital characters of the states are described in Sec. IV. Dashed lines denote regions where the surface states mix heavily with bulk states and with each other, and become indistinct. The reduced surface Brillouin zone is inset, with high-symmetry points shown.

zone. The surface-state notation is chosen to conform to previous tight-binding calculations on the unrelaxed reduced surface.[10] The calculated unrelaxed surface-state energies differ little from those shown in Fig. 7; the relaxation does not lower the energy of any surface state, at any point in k space, by more than 0.2 eV. This is because significant rehybridization of the surface atoms is prevented by the topology of the (110) surface (see the preceding section). This is in sharp contrast to some surfaces, such as (110) surfaces of various zinc-blende-structure compounds, whose topologies do allow bond-length-conserving surface atomic displacements. Such materials will often display a surface-state lowering on the order of 1.0 eV as the surface atoms rehybridize.[22]

In both panels of Fig. 7, the character of the S_1 and S_2 states is that of surface-layer tin s orbitals. The B_1 and B_2 states, located in the belly gap, are hybrids of tin s and oxygen p orbitals. The dashed lines indicate regions where the states begin to mix heavily with projected bulk states, and are therefore difficult to identify.

Surface states denoted by P_1 through P_6 are made up of surface-layer and bridging oxygen p orbitals. In the reduced surface [Fig. 7(a)], which has no bridging oxygen atoms, the P_6 state is composed of surface-layer oxygen p orbitals oriented normal to the surface plane. P_2 and P_3 project mainly along p orbitals oriented within the surface plane. For the stoichiometric surface [Fig. 7(b)], P_1 contains hybrids of p orbitals, oriented parallel to the surface plane, of bridging and surface-layer oxygen atoms. The bridging oxygen components are larger at Γ, while the surface-layer components are larger at all the other symmetry points. P_2 and P_4 are made up primarily of in-plane bridging oxygen p orbitals, while P_3 consists of bridging oxygen p orbitals oriented normal to the surface plane. Again, dashed lines indicate regions where the surface states mix heavily with each other, and with bulk states, and become indistinct.

These results, like the density-of-states calculations, indicate the absence of surface states in the fundamental band gap of cassiterite. This result is consistent with UPS measurements of the stoichiometric surface[11] [Fig. 6(b)] and previous calculations on the unrelaxed reduced surface.[10] While photoemission[8,11] and ion-scattering[8] spectroscopy on the reduced surface show appreciable densities of occupied states in the gap, these states are believed to arise from surface defects.

V. SUMMARY

Tight-binding total-energy calculations on the reduced and stoichiometric cassiterite (110) surfaces display a small, but significant relaxation of the surface atomic positions. The extent of the relaxations are constrained by the topology of the rutile-structure (110) surface, which forbids bond-length-conserving displacements of the surface atoms. The large strain fields created by bond compression prevent the surface atoms from fully rehybridizing. Consequently, the surface-state energy lowering from the relaxation is small. However, the calculated surface atomic relaxations are sufficiently large to be detected by LEED intensity analysis. The calculated density of states is in qualitative agreement with previous experimental photoemission studies of the stoichiometric surface. Moreover, results for both the reduced and stoichiometric surfaces indicate that neither surface has surface states which lie within the fundamental band gap of cassiterite.

ACKNOWLEDGMENTS

We are indebted to A. J. Skinner, David L. Blanchard, Jr., and D. L. Lessor for helpful discussions during this study. The Pacific Northwest Laboratory is operated for the U.S. Department of Energy by Battelle Memorial Institute under Contract No. DE-AC06-76RLO 1830.

[1]F. J. Berry, Adv. Catal. **30**, 97 (1982).
[2]M. del Arco, M. J. Holdago, C. Martin, and V. Rives, Mater. Sci. Forum **25/26**, 479 (1988).
[3]S. Semancik and D. F. Cox, Sens. Actuat. **12**, 101 (1987).
[4]W. Gopel, U. Kirner, H. D. Wiemhofer, and G. Rocker, Solid State Ion. **28-30**, 1423 (1988).
[5]S. Semancik and R. E. Cavicchi, Thin Solid Films **206**, 81 (1991).
[6]B. G. Hyde and Sten Andersson, *Inorganic Crystal Structures* (Wiley, New York, 1989).
[7]E. de Fresart, J. Darville, and J. M. Gilles, Surf. Sci. **126**, 518 (1983).
[8]D. F. Cox, T. B. Fryberger, and S. Semancik, Phys. Rev. B **38**, 2072 (1988).
[9]D. F. Cox and T. B. Fryberger, Surf. Sci. Lett. **227**, L105 (1990).
[10]S. Munnix and M. Schmeits, Phys. Rev. B **33**, 4136 (1986).
[11]R. G. Egdell, S. Eriksen, and W. R. Flavell, Solid State Commun. **60**, 835 (1986).
[12]J. C. Slater and G. F. Koster, Phys. Rev. **94**, 1498 (1954).
[13]D. J. Chadi and M. Cohen, Phys. Rev. B **8**, 5747 (1973).
[14]J. Robertson, J. Phys. C **12**, 4767 (1979).
[15]T. J. Godin and John P. LaFemina, in *Structure and Properties of Interfaces in Materials,* edited by W. A. T. Clarke, U. Dahmen, and C. L. Bryant (Materials Research Society, Pittsburgh, 1992); T. J. Godin and John P. LaFemina, in *Computational Methods in Materials Science,* edited by J. E. Mark, M. E. Glicksman, and S. P. Marsh (Materials Research Society, Pittsburgh, 1992).
[16]Walter A. Harrison, *Electronic Structure and the Properties of Solids,* 2nd ed. (Dover, New York, 1989).
[17]R. Feynman, Phys. Rev. **56**, 340 (1939).
[18]John P. LaFemina, Surf. Sci. Rep. **16**, 133 (1992).
[19]A. Kahn, Surf. Sci. Rep. **3**, 193 (1980).
[20]D. J. Chadi, J. Vac. Sci. Technol. **15**, 1244 (1978).
[21]D. A. Shirley, Phys. Rev. B **5**, 4709 (1972).
[22]C. B. Duke, in *Surface Properties of Electronic Materials,* edited by D. A. King and D. P. Woodruff (Elsevier, Amsterdam, 1992).